Measurement of Anomalous Ion Thermal Transport Due to the Ion-Temperature-Gradient Driven Instability

B. Song, J. Chen, and A. K. Sen
Plasma Physics Laboratory, Columbia University, New York, New York 10027
(Received 14 January 1993)

The anomalous ion thermal transport due to the ion-temperature-gradient driven instability (ITG mode) has been studied in the Columbia Linear Machine. We find that in the presence of the ITG mode, the radial temperature profile relaxes along the direction of a steady state plasma flow parallel to the magnetic field lines. The corresponding local ion thermal conductivity $\chi_\perp(r)$, determined from the experimental data, is highly anomalous and shows a strong correlation with the radial profile of the ITG mode.

PACS numbers: 52.35.Kt, 52.35.Mw

A number of recent experiments [1-4] have shown that anomalous ion thermal transport is an important aspect of energy confinement in large tokamaks. The theoretical studies [5-7], as well as experimental investigations [1-4], suggested that ion-temperature-gradient driven instabilities (ITG mode) may be responsible for the thermal loss. However, the recent experiments designed to verify this scenario in the TFTR raised some uncertainties [8]: In contrast to the theoretical prediction, the radial thermal flux did not increase while the parameter η_i $(=d\ln T_i/d\ln n_i)$, characterizing the strength of the ITG mode drive, increased significantly. There have been recent theoretical attempts to reconcile these experimental results with refined theoretical models [9,10]. Therefore, the transport due to the ITG mode remains a partly open question. The slab branch of the ITG mode has been recently produced by two different methods and definitively identified in the Columbia Linear Machine (CLM) [11,12]. The objective of the present research was to measure the anomalous ion thermal diffusion induced by the slab branch of the ITG mode which may be relevant to the thermal confinement in tokamaks and other toroidal confinement devices.

The layout of the CLM is shown in Fig. 1. The plasma is produced in the source region by a hot-cathode dc discharge ($V_{\rm dis}=45$ V, $I_{\rm dis}=80$ mA) in hydrogen ($P_s\cong 5\times10^{-4}$ torr) [13]. The plasma flows from the source region through a differentially pumped transition region to the experimental cell ($P_c\approx 5\times10^{-7}$ torr) where the plasma terminates on a conducting end plate. The rf heating meshes, located at the transition region, effectively heated the core of the plasma in the parallel direction so that an ITG mode was excited. The details of the rf heating technique have been described in Ref. [12]. The typical parameters under normal operating conditions with a rf heating are as follows: ion density $n_i\sim5\times10^8$ cm^{-3}, neutral pressure in cell region $P_c\approx5\times10^{-7}$ torr, electron temperature $T_e\sim10$ eV, perpendicular ion temperatures $T_{i\perp}\sim5$ eV, parallel ion temperatures $T_{i\parallel}\sim15$ eV, $\eta_{i\parallel}\sim6$, $\eta_{i\perp}\leq1$, magnetic field (experimental cell) $\mathbf{B}\approx1$ kG, plasma cell length $L\sim160$ cm, and plasma column $r_p\sim3$ cm.

The parallel and transverse ion temperatures were measured with gridded ion energy analyzers. Rectangular Langmuir probes (2 mm×5 mm) were used to obtain electron temperatures and ion saturation current and to detect density fluctuations. The plasma potential was obtained from the floating potential of an emissive probe. These electrostatic probes are fixed at axial positions but could be moved radially to obtain profiles of the various plasma parameters.

Figure 2 shows the frequency spectra for the cases with and without rf heating of ions. Without heating (dashed curve), $\eta_{i\parallel}<1$, which is less than the critical value for the onset of the instability, so the fluctuation level is low. However, when the heating is turned on and $\eta_{i\parallel}\sim6$, two features appear. The mode with frequency $f\sim95$ kHz has been identified as an ITG slab mode with an azimuthal mode number $m=2$ and the other one ($\mathbf{E}\times\mathbf{B}$ mode) with frequency $f\sim55$ kHz and $m=1$ is believed to be a Rayleigh-Taylor type instability, driven by $\mathbf{E}\times\mathbf{B}$ rotation of the plasma column [11,12]. The experimental conditions for this case have been carefully adjusted such that the $\mathbf{E}\times\mathbf{B}$ mode is minimized leaving the ITG mode to be the principal instability responsible for the observed ion

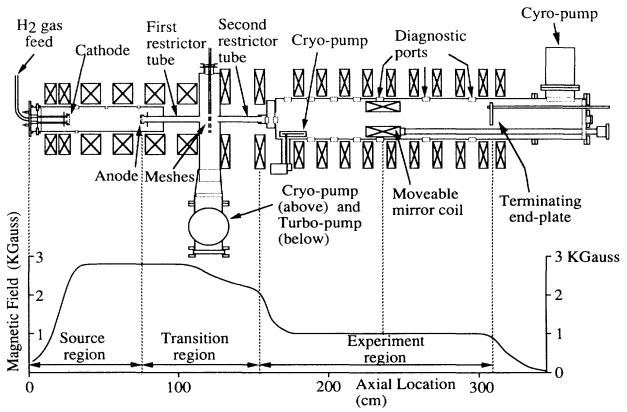

FIG. 1. Layout of the Columbia Linear Machine. The relative positions for the heating meshes, ion energy analyzer, and end plate are shown in the figure.

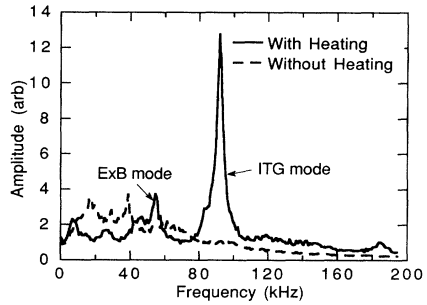

FIG. 2. Frequency spectra at $r=2.0$ cm with and without heating. The plasma conditions: end plate voltage $V_{ep}=5.0$ V, neutral pressure at the experimental cell $P_c=4\times10^{-7}$ torr, rf heating voltage $V_{rf}=45$ V, and magnetic field in the cell region $\mathbf{B}=1.0$ kG.

thermal transport.

The ITG instability produced in the transition region, where a sharp temperature gradient is created, travels down the machine with the plasma flow as shown in Fig. 3. The mode is nonlinearly saturated and the ITG turbulence is fully developed by the time it reaches the experimental cell. The ions experience the ITG turbulence scattering as they flow down the machine and enhanced ion thermal transport may be produced. A significant mode fluctuation level exists between $z=60$ cm (upstream) and $z=125$ cm (downstream) where the transport experiments were conducted, because the value of $\eta_{i\parallel}$ is variable but larger than the critical value $\eta_{i,\mathrm{crit}}$ over this whole range. Two ion energy analyzers or Langmuir probes, calibrated against each other, are located at $z=65$ cm and $z=125$ cm (see Fig. 3). The position of the heating mesh is taken as $z=0$ cm. Therefore, the subsequent particle diffusion or thermal transport can be measured by determining the ion density and ion temperature radial profile relaxation downstream.

The transverse particle diffusion (across **B** field lines), which can cause thermal convection, was carefully studied by measuring both upstream and downstream ion

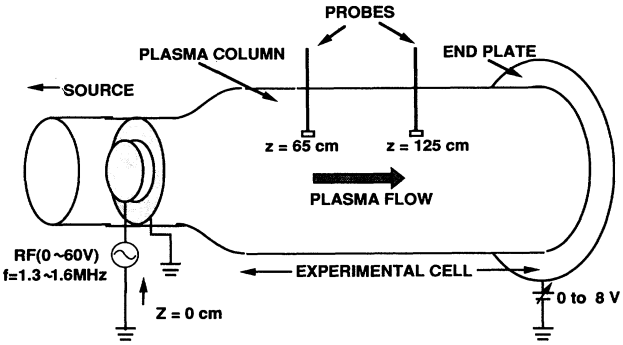

FIG. 3. Schematic of the temperature relaxation measurement scheme.

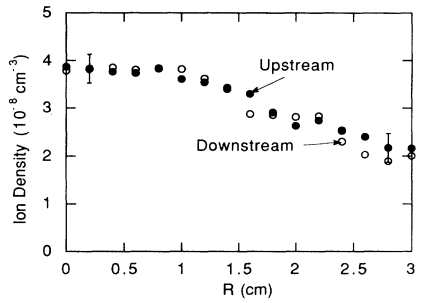

FIG. 4. Both upstream and downstream ion density profiles.

density profiles. Figure 4 shows the results with the presence of the ITG mode. No significant density profile relaxation is observed. Therefore, the thermal convection could be neglected. This is consistent with the presumption that the electron density response is approximately adiabatic for the ITG mode in CLM. The fluctuations of the density and the radial velocity are 90° out of phase in the adiabatic approximation and no particle transport can result.

The radial ion temperature profiles at $z=65$ cm and $z=125$ cm for both cases with and without the ITG modes are displayed in Fig. 5. Without the mode [Fig. 5(a)], both upstream and downstream temperature profiles are roughly the same. With the mode [Fig. 5(b)], the temperature relaxation is obvious. The profile relaxation is a result of heat flux direct from the plasma center to the edge, causing the plasma core ($r<2.0$) to cool

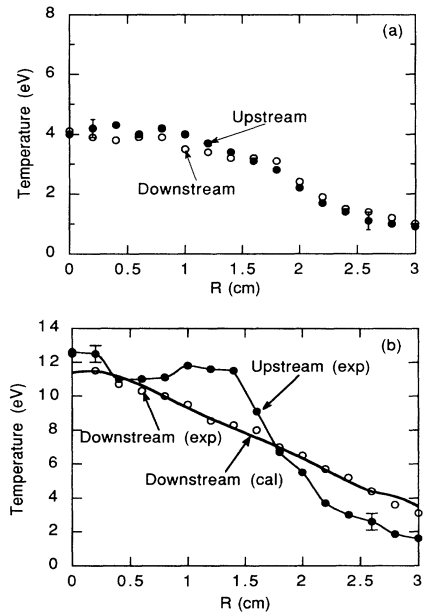

FIG. 5. Ion temperature profiles for both upstream and downstream: (a) without heating; (b) with heating.

down and the plasma edge ($r > 2.0$) to heat up. Because no particle transport is observed, transverse thermal convection can be neglected. Therefore, the observed ion thermal transport shown in Fig. 5(b) is dominated by the thermal conduction.

We now model the temperature profile relaxation and calculate the transverse ion thermal conductivity $\chi_\perp$. While the anomalous transverse ion thermal conduction is very important as discussed above, the anomalous (wave-induced) parallel ion thermal conduction (parallel to the **B** field) is insignificant in our experiment. This is because compared with the perpendicular wavelength $\lambda_\perp \sim 3$ cm, the parallel wavelength $\lambda_\parallel \sim 500$ cm is very long so that the ITG modes mix the hot and cold ions perpendicular to the **B** field only. Furthermore, since the plasma in CLM is collisionless, the thermal conduction due to the classical collisions is entirely negligible. Therefore, the ion energy transfer along the **B** field is basically determined by the plasma flow. As the transverse thermal convection can be neglected in accordance with the discussion above, the radial ion thermal flux is entirely due to the transverse thermal conduction, i.e., $\mathbf{q} = -n_i \chi_\perp \nabla T_{i\parallel}$, where $\mathbf{q}$, $\chi_\perp$, n_i, and $T_{i\parallel}$ are ion thermal flux across the **B** field line, transverse ion thermal conductivity, ion density, and parallel ion temperature, respectively. Then in the steady state the transport equation governing the ion temperature relaxation can be written as follows:

$$n_i v_f \frac{\partial}{\partial z} T_{i\parallel} = \frac{1}{r} \frac{\partial}{\partial r} \left(r n_i \chi_\perp \frac{\partial}{\partial r} T_{i\parallel} \right), \quad (1)$$

where v_f is the plasma flow velocity. The physical meaning of the above equation is clear: The energy input via parallel thermal convection (left side of the equation) is balanced with the energy output via the transverse thermal conduction (right side of equation) so that there is ion energy balance in steady state in the laboratory frame. Because the ion temperature and ion density profiles are known and plasma flow velocity can be measured by launching ion acoustic waves, Eq. (1) can be solved to obtain $\chi_\perp$. The measurement of the velocity was carried out by launching ion acoustic waves along the magnetic field **B**, i.e., parallel to the flow velocity [14]. The waves propagating in the plasma flow direction result in a phase velocity $v_1 = v_s + v_f$ in the laboratory frame while the waves propagating in the opposite direction yield $v_2 = v_s - v_f$, where v_s is the ion acoustic velocity. Therefore, the flow velocity v_f can be determined from $v_f = (v_1 - v_2)/2$. For the experimental conditions, we get $v_f \sim 1.5 \times 10^6$ cm/s and $v_s \sim 6 \times 10^6$ cm/s. The value of v_s is consistent with that calculated from the ion and electron temperatures and the value of v_f is consistent with the existence of a substantial fraction of electrostatically trapped ions due to the positive end plate bias (+5 V). Equation (1) is numerically solved by the explicit finite difference method [15]. Since no experimental data are available outside $r = 3.0$ cm, an exponentially decaying function is assumed in this region. The temperature profile at $z = 65$ cm [Fig. 5(b)] is chosen as the upstream boundary condition. As a result of the negligible transverse particle transport, the density profile at $z = 65$ cm, fitted by an eighth order polynomial, is used in the equation. The thermal conductivity $\chi_\perp(r)$ is modeled by a trial function with a number of adjustable parameters such that the calculated temperature profile at $z = 125$ cm is optimally fitted to the experimental downstream temperature. The decay of the ITG mode amplitude in z will have some effect on the measured $\chi_\perp$. However, we can only scan the temperature at two axial positions ($z = 60$ cm and 125 cm); the simplest model we can use is a conduction equation with a constant $\chi_\perp$ in z. Therefore, the thermal conductivity $\chi_\perp$ determined in this manner should be considered to be a z averaged but radially local $\chi_\perp(r)$. The details of the numerical method will be published later. The calculated temperature profile is displayed in Fig. 5(b) (solid curve). The fit of the calculated profile to the experimental profile is fairly good. The corresponding ion thermal conductivity is shown in Fig. 6. It is noted that the position of the maximum thermal conductivity is around the location of the maximum temperature gradient. More interestingly, it also corresponds to the peak of the ITG mode amplitude as shown in Fig. 6. The radial profile of the ITG mode can be compared with the calculated thermal conductivity which indicated remarkable similarity. The conductivity is small at the center where the fluctuation level is also low. Therefore it can be concluded that the measured thermal conductivity is due to the ITG mode.

We note that the average thermal conductivity (~ 0.5 m^2/s) is much larger than the classical ($\sim 10^{-3}$ m^2/s) and less than the Bohm diffusion coefficient (~ 6 m^2/s). For the CLM parameters, the quasilinear theory yields $\chi_\perp \sim 0.5$ m^2/s [7], the Kadomtsev strong turbulence estimate gives $\chi_\perp \sim 1$ m^2/s [16], and by considering the invariance properties of the fluid equations, $\chi_\perp \sim 2$ m^2/s is obtained [6].

In conclusion, the anomalous ion thermal transport due

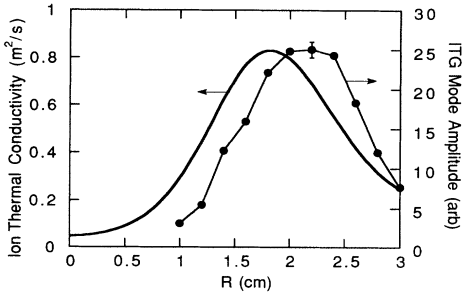

FIG. 6. The radial profiles of ion thermal conductivity determined from the data shown in Fig. 5 and the measured ITG mode amplitude.

to the ITG mode has been measured in the CLM by the temperature profile relaxation method. The ITG mode does cause significant anomalous ion thermal transport across magnetic field lines primarily via thermal conduction. The local ion thermal conductivity $\chi_\perp(r)$, determined from the experimental data, shows a strong correlation with the ITG mode radial profile and its magnitude is about an order of magnitude lower than Bohm.

The authors acknowledge fruitful discussion with P. Tham. This research was supported by U.S. Department of Energy Grant No. DE-FG-02-87ER53257.

[1] S. M. Wolfe *et al.*, Nucl. Fusion **26**, 329 (1986).
[2] P. C. Efthimion *et al.*, Phys. Rev. Lett. **66**, 421 (1991).
[3] T. Hirayama *et al.*, Nucl. Fusion **32**, 89 (1992).
[4] D. L. Brower *et al.*, Phys. Rev. Lett. **59**, 48 (1987).
[5] G. S. Lee and P. H. Diamond, Phys. Fluids **29**, 3291 (1986).
[6] J. W. Connor, Nucl. Fusion **26**, 193 (1986).
[7] T. M. Antonsen, B. Coppi, and R. Englade, Nucl. Fusion **19**, 641 (1979).
[8] M. C. Zarnstorff *et al.*, *Conference on Controlled Fusion and Plasma Heating, Amsterdam, 1990* (European Physical Society, Petit-Lancy, Switzerland, 1990), Vol. 14B, Pt. 1, p. 42.
[9] W. Horton *et al.*, Phys. Fluids B **4**, 953 (1992).
[10] N. Mattor, Phys. Fluids B **3**, 1913 (1991).
[11] A. K. Sen, J. Chen, and M. Mauel, Phys. Rev. Lett. **66**, 429 (1991).
[12] R. G. Greaves, J. Chen, and A. K. Sen, Plasma Phys. Contr. Fusion **34**, 1253 (1992).
[13] G. A. Navratil, A. K. Sen, and J. Slough, Phys. Fluids **26**, 1044 (1983).
[14] R. W. Motley, *Q Machines* (Academic, New York, 1975).
[15] W. F. Ames, *Numerical Methods for Partial Differential Equations* (Academic, New York, 1977), 2nd ed.
[16] B. B. Kadomtsev, *Plasma Turbulence* (Academic, New York, 1965).